ACS OMEGA

Article

Cite This: ACS Omega 2018, 3, 22−29

Circular Dichroisms of Mono- and Dibromo[2.2]paracyclophanes: A Combined Experimental and Theoretical Study

Mitsunobu Toda, Yoshihisa Inoue, and Tadashi Mori*

Department of Applied Chemistry, Graduate School of Engineering, Osaka University, 2-1 Yamada-oka, Suita, Osaka 565-0871, Japan

Supporting Information

ABSTRACT: Circular dichroisms (CDs) of planar chiral 4-bromo[2.2]paracyclophane (**1**) and three isomeric dibromo[2.2]paracyclophanes (*p*-**2**, *m*′-**2**, and *o*′-**2**) were investigated experimentally and theoretically. They all exhibited strong multisignate Cotton effects (CEs) at the ^1L_b, ^1L_a, and ^1B transitions of the component (bromo)benzene chromophore and were comparable to each other. For all of the cyclophanes examined, the enantiomer that eluted earlier from a chiral high-performance liquid chromatography column (Chiralcel IA or IB) exhibited negative and positive CEs at the ^1L_b and ^1L_a bands, respectively, which were followed by a more complicated pattern of CDs at the higher-energy bands. These CD features were well reproduced by quantum chemical calculations, allowing us to unambiguously assign the absolute configurations of the first-eluted enantiomers as R_p in all of the cases examined. Interestingly, the CDs of **1** and **2**, although largely comparable in shape, were still sensitive to the number and pattern of bromine substitution, showing closer resemblance between *m*′-**2** and *o*′-**2** and between *p*-**2** and **1**. The theoretical calculations also reproduced successfully these spectral resemblance between them. The anisotropy (*g*) factors for the ^1L_b bands of these cyclophanes were considerably large (~10^{-2}), whereas those for the ^1L_a band were conventional in the order of 10^{-3}. In addition, a weak CE was observed in the low-energy region at around 320 nm, which turned out to originate from the interplanar interaction and is hence assigned to the "cyclophane band". The experimental *g* factors of this band were fairly large in the order of 10^{-2}, but the computation turned out to be quite challenging and were less well reproduced theoretically, ascribable to the forbidden nature of the transition.

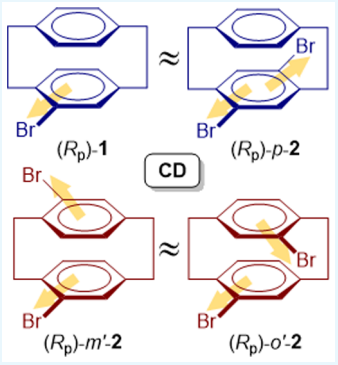

INTRODUCTION

Possessing unique planar chirality,[1−3] [2.2]paracyclophanes have been utilized in various applications, such as coordinated metal catalysts and supramolecular assemblies.[4−7] Brominated cyclophanes are versatile starting materials for the preparation of more complex cyclophane derivatives. Somewhat surprisingly, the study on the circular dichroism (CD) arising from the planar chirality of these cyclophanes is still quite limited,[8] and practically no systematic efforts have hitherto been devoted to the investigation of the chiroptical properties of substituted [2.2]paracyclophanes.[9,10] In particular, the "cyclophane band",[11] observed in the low-energy region specifically for smaller [2.*n*]cyclophanes due to the interplanar interactions, has rarely been examined comprehensively from the chiroptical viewpoint. In the present study, we compared the CD spectra of monobrominated cyclophane (**1**) as well as all of the possible C_2-symmetric chiral dibromo[2.2]paracyclophanes (*p*-**2**, *m*′-**2**, and *o*′-**2**) (see Chart 1).[12] As anticipated, all of these cyclophanes exhibited strong, mutually resembling Cotton effects (CEs) at the ^1L_b, ^1L_a, and ^1B transitions, owing to their planar chirality. Additionally, the cyclophane band appearing in the low-energy region gave appreciable CE with high anisotropy (*g*) factors in the order of 10^{-2}.

These brominated cyclophanes serve as a model system suitable for not only understanding the chiroptical consequences of planar chirality but also evaluating the strengths and

Chart 1. Planar Chiral Mono- and Dibromo[2.2]paracylophanes 1−2

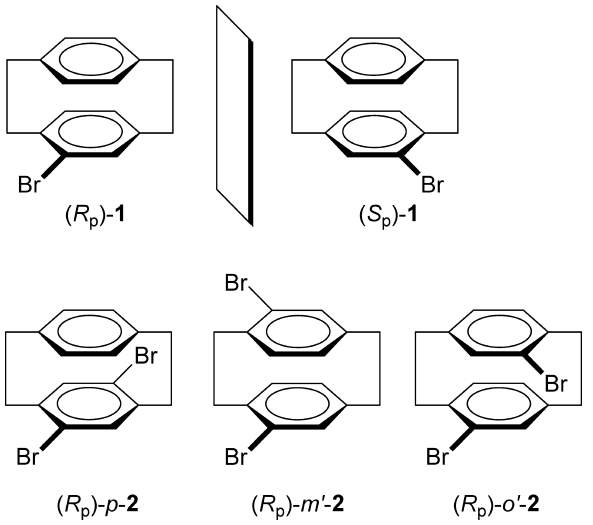

Received: October 25, 2017
Accepted: November 22, 2017
Published: January 2, 2018

DOI: 10.1021/acsomega.7b01642
ACS Omega 2018, 3, 22−29

weaknesses of the state-of-the-art theoretical CD prediction. We found that the advanced theoretical calculations successfully reproduce the characteristic experimental CD patterns in sign and order for the strong ^1L_b, ^1L_a, and ^1B transitions of **1**−**2**, allowing unambiguous determination of the absolute configurations. However, the overall reproducibility was slightly lower, when compared with the results for other rigid chiral organic molecules of similar or slightly larger sizes, due to the complicated origin of transitions associated with the interplanar $\pi-\pi$ and linker-incorporated $\sigma-\pi$ interactions in the current system. Inspection of the weak CEs at the cyclophane band will provide additional insights for better understanding the nature of the interplanar interactions in cyclophane. It turned out, however, to be more challenging to accurately reproduce the observed CEs at the cyclophane band by any of the current theoretical methods, possible reasons for which will be discussed below.

RESULTS AND DISCUSSION

Structure. The structure of [2.2]paracyclophanes has attracted much attention and has long been a target of extensive experimental and theoretical investigations.[13] The most accurate X-ray crystallographic structure of parent [2.2]paracyclophane shows twisted D_2 symmetry with a dihedral angle $\Phi_{C(Ar)-C-C-C(Ar)}$ of 12.6° and an interplane distance d of 3.10 Å (Table 1). The theoretical reproduction of [2.2]paracyclophane structure has been challenged by a number of methods, rendering this system a benchmark for assessing the accuracy of the theory employed. The standard density functional theory (DFT) with B3LYP functional failed to provide the correct structure, and the structure with D_{2h} symmetry (Φ = 0) was obtained as a minimum. Although the MP2 calculation circumvented such deficiency, it overestimated the dihedral angle (Φ = 18.7°). The situation was slightly improved using the spin-component scaled second-order Møller−Plesset (SCS-MP2)[14] method (Φ = 17.6°), which has been frequently employed as an alternative to the gold standard CCSD(T) ansatz. The recent investigation has underlined that the medium-range dispersion correction is crucial for a cost-effective, yet accurate prediction of the cyclophane structures.[15] For instance, interplane distances of various [2.2]cyclophanes can be precisely predicted with errors much less than 0.01 Å using the dispersion-corrected DFT method with Becke−Johnson (BJ) dumping function. Accordingly, we calculated the optimized geometries for all of the brominated [2.2]paracyclophanes **1**−**2** at the DFT-D3(BJ)-TPSS/def2-TZVP level,[16,17] which was quite successful indeed, affording the geometrical parameters comparable to those obtained by X-ray crystallography (Table 1). Compatibility of the theoretical method of choice with cyclophane structure has also been justified by our recent investigations on pyridinophane systems.[18−20] Because crystal structures are not available for some cyclophanes, we employed these DFT-D3-optimized structures for the following theoretical CD investigation. The parent [2.2]paracyclophane possesses a shallow double-minimum potential along the dihedral-angle coordinate (two minima at $\Phi = \pm 12.6°$). As such, the weighted average of the two conformers at the TD-DFT-B3LYP/TZV2P′//MP2/TZVP level was used to reproduce the experimental CD spectrum of 4-fluoro[2.2]paracyclophane,[8] whereas the minor conformer was missing at the B3LYP/TZVP-level geometry optimization.[21] In all of the brominated [2.2]paracyclophanes employed in this study, the twisting of ethylene bridge toward the bromine atom is avoided due to the greater steric hindrance in these brominated cyclophanes. In this relation, Grimme and Bahlmann pointed out an additional possibility in conformer structure, i.e., the parallel-displaced, rather than twisted, conformer observed in methylcyclophane thoroughly discussed previously.[8] We were unable to find the corresponding conformer in the case of brominated cyclophanes. Accordingly, a single conformer possessing a positive dihedral angle was obtained as the optimized structure for each of cyclophanes **1**−**2**. The overall twist of Φ = 8.6−18.3° in brominated cyclophanes was considerably larger than that of parent [2.2]paracyclophane, whereas the interplane distance and the degree of deformation were found quite comparable (vide infra).

Table 1. Selected Geometrical Parameters of Parent and Brominated [2.2]Paracyclophanes 1−2[a]

cyclophane	method	d (d') (Å)	α/β (deg)	Φ (deg)
PCP[b]	calc	3.08 (2.78)	11.9/11.0	7.1
		[3.08 (2.77)]	[12.2/11.5]	[17.6]
	exp[c]	3.10 (2.78)	12.5/11.0	12.6
1	calc	3.08 (2.78)	12.0/11.3	17.0/11.0
p-**2**	calc	3.08 (2.77)	12.0/11.5	17.9
m′-**2**	calc	3.08 (2.77)	11.9/11.3	18.3/8.6
	exp[d]	3.09 (2.76)	13.6/10.0	20.6/10.1
o′-**2**	calc	3.08 (2.77)	12.0/11.5	18.0
	exp[e]	3.08 (2.77)	11.5/11.8	19.4

[a]Selected structural parameters: d, the interplanar distance between the mean planes defined by the unbridged atoms of the (bromo)-benzene unit; d', the averaged distance of the two sets of the facing bridgehead atoms; α, the averaged deformation angle between the mean plane and the bridgehead atom; β, the additional deformation angle of the linker atom from the mean plane; Φ, the dihedral angle around bridgehead and linker atoms. Geometries were optimized at the DFT-D3(BJ)-TPSS/def2-TZVPP level. The values for SCS-MP2 geometry are within brackets.[13] [b]Parent [2.2]paracyclophane. [c]Ref 13. [d]Ref 22. [e]Ref 23.

Table 1 compares the characteristic structural parameters for cyclophanes **1**−**2**. The interplane distances measured at the bottom center of each boat-shaped benzene unit (d) and at the bridgehead atom (d') can be used as indices for evaluating the interplanar orbital interactions, which primarily affect the excitation energy and degree of degeneracy in CD spectrum. The boat-type deformation in each benzene unit, which is known to enhance the degeneracy in valence orbitals and increase the energy separation, is represented by the deformation angles α (for the bridgehead atom) and β (for the linker atom). Crucially, these parameters (d, d', α, and β) were essentially the same in all of the brominated [2.2]-paracyclophanes examined, indicating that the common structural features are preserved throughout the phenes employed, despite the bromine substitution. Consequently, the interplanar interactions, such as dispersion (van der Waals) and electrostatic (quadrupole−quadrupole) contributions between any two of the dibromo-, monobromo-, and unsubstituted benzene units, can be considered essentially the same for cyclophanes **1**−**2**. In other words, the electronic contribution of bromine atom(s) on the overall cyclophane structure is much less pronounced than the steric effect of bromine(s) on the ethylene linker. Accordingly, the twist angle, which is parameterized by C(Ar)−C−C−C(Ar) dihedral angle (Φ), was found fairly sensitive to the number and pattern of

DOI: 10.1021/acsomega.7b01642
ACS Omega 2018, 3, 22−29

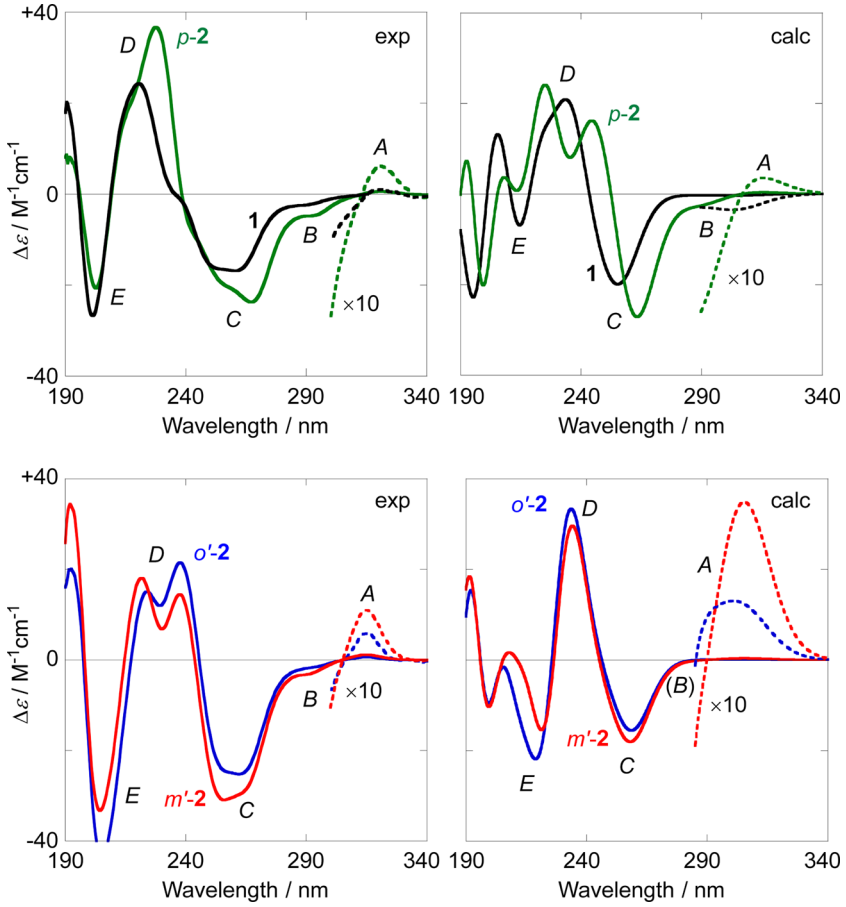

Figure 1. Experimental and calculated CD spectra of brominated [2.2]paracyclophanes **1**−**2**. Experimental spectra (left) for the first high-performance liquid chromatography (HPLC) elutes were obtained in acetonitrile at 25 °C. Theoretical spectra (right) for the R_p enantiomers were obtained at the RI-CC2/def2-TZVPP level, where the intensities are scaled to 1/3 (top) or 1/5 (bottom). The excitation energies are red-shifted by 0.2 eV to facilitate direct comparison with experiment. For the theoretical spectra with different methods, see Figure S9 in the Supporting Information.

bromine substitution. It is to note that although the formal classification defines the [2.2]paracyclophanes planar chiral, the observed CEs at the main transitions are mostly determined by the twisting between the phenes.[8] Thus, changing the twist angle is expected to significantly affect the chiroptical properties of cyclophanes. In fact, the angle becomes progressively larger by increasing the number of bromine substitution and the angle is significantly larger on the brominated side (17.0−18.3°) than on the nonbrominated side (7.1−11.0°). In brief, the structural features of cyclophanes are very well reproduced by the conventional theoretical calculations, when appropriately selected for the required accuracy. The steric, rather than the electronic, effect is more important in determining the structures of brominated paracyclophanes.

Experimental CD Spectra. The experimental CD spectra of brominated [2.2]paracyclophens **1**−**2** were obtained in acetonitrile at 25 °C (Figure 1, left). The corresponding UV−vis spectra and anisotropy ($g = \Delta\varepsilon/\varepsilon$) factor profiles are provided in Figures S5−S7 in the Supporting Information. The characteristic spectral features based on the distinctive electronic structure of [2.2]paracyclophane are apparent in their UV−vis spectra, exhibiting absorption peaks at around 270, 230, and 200 nm, which are assignable to the ^1L_a, ^1L_b, and ^1B bands, respectively. Additionally, weak absorption assignable to the cyclophane band was observed as a tail at around 310 nm, which is known as the specific transition observable only for [2.*n*]cyclophanes.[11,24,25] In parent [2.2]paracyclophane, the lowest transition of B_{2u} symmetry appears at 329 nm in single crystals at 20 K and at ≈305 nm in liquid media.[26,27] The corresponding CD peaks were observed for all of the brominated cyclophanes **1**−**2**. Accordingly, the band A with positive CE is assignable to the cyclophane band. Although the intensity of CE was relatively weak ($\Delta\varepsilon \leq 1$), the anisotropy factor was remarkably high in the order of 10^{-2}, due to the forbidden nature of this transition. Naturally, the *g* factor is dependent on both the electronic and magnetic transition moments, but the former seems more important as shown by the weak absorption in the experimental UV spectra. Theoretical analysis on the relevant transition moments was not feasible, as our current theoretical calculations could not successfully reproduce the CD spectral behavior of the cyclophane band (vide infra). The next CE of moderate strength labeled band B was not decisive, but likely to originate from the transition related to the ^1L_b transition. The bands C and D are attributed to the ^1L_b and ^1L_a transitions of phene chromophore. Their CE intensities are high and comparable to each other ($|\Delta\varepsilon| = 16-38\ M^{-1}\ cm^{-1}$), whereas the anisotropy factor differs in 1 order of magnitude between the two bands, affording $g = 10^{-3}$ for the former but much larger, 10^{-2}, for the latter. The CE at band E and the higher-energy portion of band D are mainly ascribable to the ^1B transition. It is to note that due to the complexity caused by the dense population of

DOI: 10.1021/acsomega.7b01642
ACS Omega 2018, 3, 22−29

Table 2. Experimental Cotton Effects Observed for Bromo[2.2]paracyclophanes 1−2[a]

	1		*p*-2		*m*′-2		*o*′-2	
band	λ/nm	$\Delta\varepsilon$/M^{-1} cm^{-1}	λ/nm	$\Delta\varepsilon$/M^{-1} cm^{-1}	λ/nm	$\Delta\varepsilon$/M^{-1} cm^{-1}	λ/nm	$\Delta\varepsilon$/M^{-1} cm^{-1}
A	322	+0.1	321	+0.6	316	+1.1	316	+0.6
B	290[b]	−2.4	290[b]	−4.8	290[b]	−3.3	290[b]	−1.9
C	261	−16.8	267	−23.7	265[b]	−28.7	262	−25.3
	250[b]	−15.5	250[b]	−15.7	256	−31.0	255[b]	−24.1
D	221	+24.3	228	+36.7	238	+14.4	238	+21.5
	215[b]	+19.3	215[b]	+17.2	222	+18.0	222	+15.0
E	202	−26.7	203	−20.6	205	−33.3	205	−43.6

[a]In acetonitrile at 25 °C. [b]Shoulder.

various states, the assignment of the apparent CD peak to specific transition(s) is not immediately feasible and hence our present assignment is rather tentative and may be used for a guiding purpose only. For more detailed band assignment, one can refer to the specific transition configuration through the computational results (for the examples of densely populated transitions, see the bar spectra in Figure S8 in the Supporting Information). A more precise assignment of the UV−vis spectra of unsubstituted cyclophanes can be found in the literature.[28,29]

Table 2 summarizes the CEs observed for brominated [2.2]paracyclophanes **1**−**2**, where the signs are of the first elutes from chiral HPLC. As clearly seen, all of these cyclophanes share the common characteristics, affording the identical CE signs with similar magnitudes at the closely located excitation wavelengths for all of the bands A−E. It should be stressed that the CD spectral investigation of disubstituted [2.2]paracyclophanes (although limited to the pseudo-meta-isomers) has appeared only recently.[30] The CE sign of the ^1L_b band has been correlated with the absolute configuration of substituted [2.2]paracyclophanes, assigning negative and positive CEs to R_p and S_p configurations, respectively,[31] which is theoretically validated by our calculations. Moreover, the whole CD spectral pattern was well reproduced by the theoretical calculation (vide infra), and the absolute configurations of the first HPLC elutes of all brominated cyclophanes **1**−**2** were unequivocally assigned to R_p (Figure 1).

A closer look at the experimental CD spectra (Figure 1) and their *g* factor profiles (Figure S7 in the Supporting Information) provided us with additional insights into the planar chirality of substituted cyclophanes. Although the apparent resemblance is noted among all of the brominated cyclophanes **1**−**2**, the similarity is much higher between **1** and *p*-**2** (cf. black versus green line in Figure 1) and between *m*′-**2** and *o*′-**2** (red versus blue line). The strength of observed CEs is slightly more enhanced in *p*-**2** than in **1**, except for the band E. In contrast, all CEs, but the band A, are nearly comparable in strength between *m*′-**2** and *o*′-**2**. This chiroptical behavior seems reasonable, as two exactly the same bromobenzene chromophores are aligned in the latter pair (*m*′-**2** and *o*′-**2**), whereas the facing chromophore units are not equal to each other in the former pair (**1** and *p*-**2**; see Chart 2). In the former equal chromophore pair, the relative orientation of electronic transition moments becomes nearly identical between the phenes due to the existence of C_2 axis. In the latter unequal pair, the enhanced intensity in *p*-**2** is explained by the additional bromine substituent introduced to **1**. It is also to stress that the geometrical similarity is not a determining factor, as the cyclophanes are more resembling between **1** and *m*′-**2** and between *p*-**2** and *o*′-**2** in terms of the twist angle Φ (Table 1). The observed CD spectra, however, are not simply explained by

Chart 2. Relative Orientation of Electronic Transition Moments (Red: Bromo- or Dibromobenzene; Blue: Benzene) in Mono- and Dibrominated[2.2]paracyclophanes 1−2, Emphasizing the Unequal (Left) and Equal (Right) Chromophore Pairs Involved

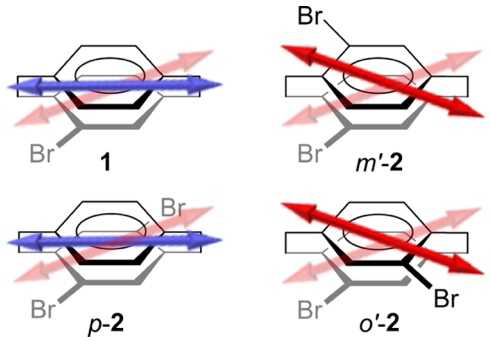

the conventional excitonic coupling between the two substituted benzene chromophores.[32,33] Due to the effective $\sigma-\pi$ interaction with the bridging linker, the relevant orbitals are degenerated to afford a more complex mixture of states.[34] The cyclophane band is described by exciton and charge resonance interactions between the two facing phenes.[25,27] Thus, the apparent difference in the CD shapes of **1** and *p*-**2** and of *m*′-**2** and *o*′-**2** pairs is ascribable to the altered energy splitting of relevant orbitals due to the different interplanar interaction between the phenes. It is reasonable that the strengths of CEs in dibromocyclophanes are always comparable, as the number of bromine atoms or the steric hindrance derived therefrom is a decisive factor for the cyclophane structure (i.e., dihedral angle Φ) rather than the electronic factor. The CE at the cyclophane band was almost negligible in **1** ($\Delta\varepsilon$ = +0.1 M^{-1} cm^{-1}), which was enhanced to +0.6 M^{-1} cm^{-1} for *p*-**2** and *o*′-**2**. This was doubled to +1.2 M^{-1} cm^{-1} in *m*′-**2**, where both the bromine atoms are located adjacent to the same linker chain, which affects the associated $\sigma-\pi$ interaction more rigorously, leading to the higher anisotropy for this transition.

Theoretical Investigation. When the theoretical calculation successfully reproduces the experimental CD, all of the associated estimates, including geometry, excitation energy, and rotational strength, are well reproduced in required accuracy. With such a calculation result, one can also extract a breadth of information regarding the molecular orbital, electron/charge distribution, energy contribution, intramolecular interaction, and so on. To better interpret the observed CD spectra by theory, we employed the approximate second-order coupled cluster approach and the algebraic diagrammatic construction scheme that combines perturbation theory with configuration

DOI: 10.1021/acsomega.7b01642
ACS Omega 2018, 3, 22−29

Table 3. Calculated Excitation Energy, Oscillator Strength, and Rotatory Strength for First Three Transitions in Brominated [2.2]Paracyclophanes 1−2[a]

cyclophane	method	E_1	f_1	R_1	E_2	f_2	R_2	E_3	f_3	R_3
1	RI-CC2	4.27	0.0001	−1.9	4.57	0.0008	−1.2	5.03	0.013	−86
	RI-ADC(2)	4.27	0.0001	−2.9	4.58	0.0007	−1.8	5.02	0.015	−87
	SAC-CI	3.17	0.0001	−3.2	3.55	0.002	+4.6	4.17	0.009	−74
	M06-2X	4.47	0.0001	−3.9	4.80	0.001	−1.0	4.96	0.012	−83
	CAM-B3LYP	4.46	0.0002	−4.8	4.78	0.001	−4.8	4.91	0.010	−39
	BHLYP	4.54	0.0003	−7.6	4.82	0.002	−20	4.96	0.006	−15
p-**2**	RI-CC2	4.19	0.0002	+2.8	4.50	0.001	−13	4.91	0.031	−98
	RI-ADC(2)	4.19	0.0001	+1.8	4.50	0.001	−14	4.89	0.041	−109
	SAC-CI	3.11	0.0003	+1.4	3.48	0.001	−6.6	4.04	0.028	−83
	M06-2X	4.43	0.0006	+3.5	4.71	0.002	−27	4.88	0.035	−134
	CAM-B3LYP	4.41	0.0003	+1.6	4.69	0.003	−25	4.83	0.026	−71
	BHLYP	4.50	0.0003	−1.8	4.75	0.013	−37	4.87	0.011	−49
m′-**2**	RI-CC2	4.27	0.0001	+3.5	4.54	0.0005	−1.1	4.99	0.039	−143
	RI-ADC(2)	4.27	0.0001	+2.8	4.55	0.0005	−1.3	4.98	0.041	−148
	SAC-CI	3.19	0.0001	+1.5	3.53	0.001	+0.8	4.12	0.024	−130
	M06-2X	4.50	0.0002	+6.6	4.80	0.001	−0.3	4.95	0.033	−130
	CAM-B3LYP	4.48	0.0001	+4.1	4.78	0.0001	−1.2	4.90	0.027	−64
	BHLYP	4.57	0.0001	+2.9	4.84	0.009	−23	4.95	0.015	−26
o′-**2**	RI-CC2	4.27	0.0001	+1.1	4.54	0.0001	+0.7	5.00	0.034	−132
	RI-ADC(2)	4.27	0.0001	+0.4	4.54	0.0001	+0.5	4.98	0.038	−138
	SAC-CI	3.28	0.0001	+0.1	3.61	0.001	+4.7	4.21	0.024	−124
	M06-2X	4.50	0.0002	+3.2	4.79	0.0001	+1.1	4.96	0.029	−115
	CAM-B3LYP	4.48	0.001	+1.1	4.76	0.0003	−3.6	4.92	0.023	−50
	BHLYP	4.57	0.0001	−0.6	4.83	0.007	−23	4.97	0.013	−14

[a]Calculated *n*-th excitation energy (E_n in eV), oscillator strength (f_n), and rotatory strength (R_n) at the RI-CC2/def2-TZVPP, RI-ADC(2)/def2-TZVPP, SAC-CI/def2-TZVP, or TD-DFT/def2-TZVP level. Excitation energies and intensities were not shifted or scaled.

interaction, both combined with the density-fitting procedure. These methods, RI-CC2[35] and RI-ADC(2)[36] methods for short, have been successfully used recently for reproducing the CD spectra of various molecular and supramolecular systems.[37−43] Practically, these are often the only available options, where simulation with more familiar time-dependent density functional theory (TD-DFT) method fails. Indeed, both methods successfully predicted the comparable spectra for **1** and *p*-**2** and for *m*′-**2** and *o*′-**2**, in nice agreement with the experimental observations (Figure 1, right, see also Figure S9 in the Supporting Information). The characteristic pattern in each pair was well predicted by theory, but the individual (apparent) transition bands were not reproduced at a level of accuracy that we commonly achieved in other cases.[37,38,43] For a comparison purpose, we also employed the symmetry-adapted cluster configuration interaction (SAC-CI)[44] method as well as the cost-efficient TD-DFT[45] method with several representative functionals, including the global and range-separated hybrid functionals, Becke's half-and-half nonlocal exchange combined with the Lee−Yang−Parr correlation functionals (BHLYP),[46] the hybrid meta-exchange−correlation functionals of Truhlar and Zhao (M06-2X),[47] and the long-range corrected hybrid exchange−correlation functional (CAM-B3LYP).[48] They all provided comparable CE patterns with slight deviations in CD intensity and/or excitation energy at the main bands, except for the cyclophane band (Figure S9 in the Supporting Information). A somewhat better performance has been observed with the SAC-CI method in describing the chirality of a low-energy band of dichlorodiphenyltrichloroethane and dichlorodiphenyldichloroethane,[43] but was not the case in the present systems. Furthermore, the excitation energies were considerably underestimated by this method. Among three functionals in the TD-DFT method, the M06-2X method outperformed in overall reproducibility for all of the cyclophanes examined here, but in general, the TD-DFT method is not recommended for accurate prediction of the CD spectra of planar chiral cyclophanes. Nevertheless, direct comparison of the calculated spectra with the experimental counterparts allows us to unambiguously determine the absolute configurations of planar chirality of brominated [2.2]paracyclophanes **1**−**2** as R_p for the first HPLC elutes.

Because both the RI-CC2 and RI-ADC(2) provided essentially the same results and outperformed any of the TD-DFT and SAC-CI methods, we focus on the results obtained by the RI-CC2/def2-TZVPP method here (Figure 1, right). For better comparison with the experimental spectra, the calculated spectra were scaled to 1/3 for **1** and *p*-**2** or to 1/5 for *m*′-**2** and *o*′-**2**, typical corrections frequently employed for other cyclophane systems.[18−20] Such scaling against experiment was always observed in this level of calculation, and presumably due, at least in part, to the possible ignorance of molecular dynamic behavior as well as vibronic contributions, but certainly requires further development in theory.

In the former pair, bands A and B were properly reproduced for *p*-**2** by theory but not for **1** for reasons not clear at present. The strong negative CE at band C was well reproduced, but two transitions predicted by theory were less separated in energy and were essentially overlapped. Such disagreement in excitation energy was more apparent for the band D of *p*-**2**, which apparently exhibited double maxima in theoretical spectrum, but overlapped in experiment. The overall performance was even worse for band E, where transitions are severely overlaid, and additional peaks were noted in theory. For the latter pair, band A was slightly overestimated in intensity and

DOI: 10.1021/acsomega.7b01642
ACS Omega 2018, 3, 22−29

band B was not observed well. Both bands C and D were properly reproduced, but the experimentally observed energy splitting was not apparent in the theoretical spectra. For band E, additional peaks were overlaid in theory. It is to note that such observations were shared by *o*′-**2** and *m*′-**2**.

Table 3 numerically compares the first three low-energy transitions (including the cyclophane band and the ^1L_b transition) of brominated [2.2]paracyclophanes **1**−**2** calculated by a variety of theoretical methods. The treatment of these transitions is relatively straightforward due to the reduced complexity of possible mixing, changed order, and/or missing transitions, which often complicate the analysis in higher-energy regions. The very weak positive CE at band A observed for monobromocyclophane **1**, however, was not correctly reproduced by any of the examined calculations, all of which predicted a weak negative CE as the lowest-energy transition. This may be related to the severely forbidden nature of this transition, the calculated oscillator strength being far less than 0.0001, which is in accord with the experimental UV−vis spectral observation. The relative intensity of CE and the sign of the cyclophane band (band A) were properly predicted for all of the dibromocyclophanes by both the RI-CC2 and RI-ADC(2) methods, where improved oscillator strengths were observed. The TD-DFT method with M06-2X and CAM-B3LYP functionals afforded better results, at least the correct signs, but that with the BHLYP functional did not provide any satisfactory clue. The prediction of band B was most challenging and generally not well reproduced by any examined methods. The CEs at band C, which corresponds to the ^1L_b transition, were well reproduced by most of the theories for all cyclophanes **1**−**2**, but the TD-DFT with CAM-B3LYP and BHLYP functionals considerably underestimated the CE intensity.

The CE in the low-energy region is known to be very sensitive to the conformation of cyclophanes, as these transitions are associated with the states affected by the strong $\sigma-\pi$ interaction of the linker.[8] These unsatisfactory theoretical results would be ascribed at least in part to our failure to include the parallel-displaced conformer or other minor conformers with various dihedral angles that are thermally populated across the shallow dihedral-angle coordinate and/or to the improper estimation through the single-referenced theoretical ansatz, which is insufficient to describe the complex transitions with interplanar interaction between phenes with severe deformation. Thus, further experimental and theoretical investigations are certainly needed to fully comprehend the chiroptical behavior of the cyclophane band.

CONCLUSIONS

In this study, we investigated the chiroptical properties of mono- and dibromo[2.2]paracyclophanes **1**−**2** experimentally and theoretically. All of the cyclophanes exhibited a common characteristic pattern of strong Cotton effects in the CD spectra, owing to their planar chirality. In addition, a weak but distinctive CE was also observed in the lowest-energy region due to the interplanar interaction and is assignable to the cyclophane band characteristic to [2.*n*]cyclophanes. In-depth analysis revealed that these cyclophanes can be grouped into two different families. Thus, the detailed pattern and relative intensity of CEs are more resembling between cyclophanes **1** and *p*-**2** and between *m*′-**2** and *o*′-**2**, which is attributable not to the subtle differences in cyclophane structure but to the pattern of bromine substitution.

Theoretical calculations of the CDs of these cyclophanes were successful to properly reproduce the characteristic pattern (and the above resemblance) of the strong CEs in the main bands, which also allowed effective and unambiguous determination of the absolute configurations of planar chiral cyclophanes **1**−**2**, i.e., the enantiomers that elute earlier from Chiralcel IA or IB column are R_p without any exceptions.

In contrast, predicting CEs of the cyclophane band with a comparable accuracy turned out to be more challenging, most probably due to the severe interplanar interaction. The CEs at the cyclophane band calculated for dibromocyclophanes **2** were reasonable at least in relative strength, but that for simpler 4-bromo[2.2]paracyclophane **1** was not well reproduced. Despite the relatively simple model systems exploited for the investigation of planar chirality of cyclophane, we still encountered the unexpected chiroptical responses for the most intriguing cyclophane band, i.e., none of the state-of-the-art theoretical calculations, including RI-CC2, RI-ADC(2), SAC-CI, and TD-DFT methods, could properly reproduce its chiroptical properties. This fact urges us to further scrutinize the chiroptical properties of the cyclophane band both experimentally and theoretically by employing a wider variety of [2.*n*]cyclophanes and more accurate theoretical calculations to comprehend the nature and behavior of planar chirality.

MATERIALS AND METHODS

Racemic 4-bromo[2.2]paracyclophane **1** was commercially available (Strem Chemicals). Racemic dibromo[2.2]-paracyclophanes (*p*-**2**,[49] *m*′-**2**,[50] and *o*′-**2**[50]) were prepared as described in the literature. Optical resolution of each cyclophane was achieved by chiral HPLC on Chiralcel IA or IB column (Figures S1−S4 in the Supporting Information). For clarity, the CD spectra of first HPLC elutes are reported and discussed throughout the work; the absolute configurations of these cyclophanes were assigned as R_p by comparing the experimental and theoretical CD spectra (vide infra). Details of the spectral measurement as well as the computation can be found in the Supporting Information.

ASSOCIATED CONTENT

Supporting Information

The Supporting Information is available free of charge on the ACS Publications website at DOI: 10.1021/acsomega.7b01642.

Experimental and theoretical details and extended spectral data (PDF)

AUTHOR INFORMATION

Corresponding Author

*E-mail: tmori@chem.eng.osaka-u.ac.jp.

ORCID

Tadashi Mori: 0000-0003-3918-0873

Notes

The authors declare no competing financial interest.

ACKNOWLEDGMENTS

Financial supports from Grant-in-Aids for Scientific Research, Challenging Exploratory Research, Promotion of Joint International Research (Fostering Joint International Research), and on Innovative Areas "Photosynergetics" (Grant Numbers JP15H03779, JP15K13642, JP16KK0111, and JP17H05261)

DOI: 10.1021/acsomega.7b01642
ACS Omega 2018, 3, 22−29

and from JSPS, Asahi Glass Foundation, and Cosmetology Research Foundation are greatly appreciated.

REFERENCES

(1) Mori, T.; Inoue, Y. Recent Theoretical and Experimental Advances in the Electronic Circular Dichroisms of Planar Chiral Cyclophanes. *Top. Curr. Chem.* **2011**, *298*, 99−128.

(2) Grimme, S.; Harren, J.; Sobanski, A.; Vögtle, F. Structure/Chiroptics Relationships of Planar Chiral and Helical Molecules. *Eur. J. Org. Chem.* **1998**, *1998*, 1491−1509.

(3) Cram, D. J.; Cram, J. M. Cyclophane Chemistry: Bent and Battered Benzene Rings. *Acc. Chem. Res.* **1971**, *4*, 204−213.

(4) Paradies, J. [2.2]Paracyclophane Derivatives: Synthesis and Application in Catalysis. *Synthesis* **2011**, 3749−3766.

(5) Rowlands, G. J. The Synthesis of Enantiomerically Pure [2.2]Paracyclophane Derivatives. *Org. Biomol. Chem.* **2008**, *6*, 1527−1534.

(6) Bräse, S.; Dahmen, S.; Hoefener, S.; Lauterwasser, F.; Kreis, M.; Ziegert, R. E. Planar and Central Chiral [2.2]Paracyclophanes as Powerful Catalysts for Asymmetric 1,2-Addition Reactions. *Synlett* **2004**, 2647−2669.

(7) Elacqua, E.; Friscic, T.; MacGillivray, L. R. [2.2]Paracyclophane as a Target of the Organic Solid State: Emergent Properties via Supramolecular Construction. *Isr. J. Chem.* **2012**, *52*, 53−59.

(8) Grimme, S.; Bahlmann, A. Electronic Circular Dichroism of Cyclophanes. In *Modern Cyclophane Chemistry*; Gleiter, R., Hopf, H., Eds.; Wiley-VCH Verlag GmbH & Co. KGaA: Weinheim, 2004; pp 311−336.

(9) Rosini, C.; Ruzziconi, R.; Superchi, S.; Fringuelli, F.; Piermatti, O. Circular Dichroism Spectra (350-185 nm) of a New Series of 4-Substituted [2.2]Paracyclophanes: A Quantitative Analysis within the DeVoe Polarizability Model. *Tetrahedron: Asymmetry* **1998**, *9*, 55−62.

(10) Nugent, M. J.; Weigang, O. E., Jr. [2.2]Paracyclophane System Optical Activity. II. Circular Dichroism of Ring-Substituted Paracyclophanes. *J. Am. Chem. Soc.* **1969**, *91*, 4556−4558.

(11) Cram, D. J.; Allinger, N. L.; Steinberg, H. Macro Rings. VII. The Spectral Consequences of Bringing Two Benzene Rings Face to Face. *J. Am. Chem. Soc.* **1954**, *76*, 6132−6141.

(12) See also: Shibahara, M.; Watanabe, M.; Miyazaki, T.; Goto, K.; Matsumoto, T.; Shinmyozu, T. Synthesis of Dibromo[3.3]paracyclophanes. *Synthesis* **2016**, *48*, 1197−1201.

(13) Grimme, S. On the Importance of Electron Correlation Effects for the π-π Interactions in Cyclophanes. *Chem. - Eur. J.* **2004**, *10*, 3423−3429.

(14) Grimme, S. Accurate Calculation of the Heats of Formation for Large Main Group Compounds with Spin-Component Scaled MP2 Methods. *J. Phys. Chem. A* **2005**, *109*, 3067−3077.

(15) Grimme, S.; Mück-Lichtenfeld, C. Accurate Computation of Structures and Strain Energies of Cyclophanes with Modern DFT Methods. *Isr. J. Chem.* **2012**, *52*, 180−192.

(16) Grimme, S.; Ehrlich, S.; Goerigk, L. Effect of the Damping Function in Dispersion Corrected Density Functional Theory. *J. Comput. Chem.* **2011**, *32*, 1456−1465.

(17) Tao, J.; Perdew, J. P.; Staroverov, V. N.; Scuseria, G. E. Climbing the Density Functional Ladder: Nonempirical Meta-Generalized Gradient Approximation Designed for Molecules and Solids. *Phys. Rev. Lett.* **2003**, *91*, No. 146401.

(18) Shimizu, A.; Inoue, Y.; Mori, T. Protonation-Induced Sign Inversion of the Cotton Effects of Pyridinophanes. A Combined Experimental and Theoretical Study. *J. Phys. Chem. A* **2017**, *121*, 977−985.

(19) Shimizu, A.; Inoue, Y.; Mori, T. A Combined Experimental and Theoretical Study on Circular Dichroisms of Staggered and Eclipsed Forms of Dimethoxy[2.2]-, [3.2]-, and [3.3]Pyridinophanes and Their Protonated Forms. *J. Phys. Chem. A* **2017**, *121*, 8389−8398.

(20) Shimizu, A.; Nagasaki, K.; Inoue, Y.; Mori, T. A Chiroptical Properties of Dithia[3.3]cyclophanes Composed of Anthracene and Pyridine/Pyridinium Moieties: A Combined Experimental and Theoretical Study. *Chirality* **2017**, *29*, 677−683.

(21) Abbate, S.; Lebon, F.; Gangemi, R.; Longhi, G.; Spizzichino, S.; Ruzziconi, R. Electronic and Vibrational Circular Dichroism Spectra of Chiral 4-X-[2.2]paracyclophanes with X Containing Fluorine Atoms. *J. Phys. Chem. A* **2009**, *113*, 14851−14859.

(22) Meyer-Eppler, G.; Vogelsang, E.; Benkhäuser, C.; Schneider, A.; Schnakenburg, G.; Lützen, A. Synthesis, Chiral Resolution, and Absolute Configuration of Dissymmetric 4,12-Difunctionalized [2.2]-Paracyclophanes. *Eur. J. Org. Chem.* **2013**, 4523−4532.

(23) Bazan, G. C.; Oldham, W. J., Jr.; Lachicotte, R. J.; Tretiak, S.; Chernyak, V.; Mukamel, S. Stilbenoid Dimers: Dissection of a Paracyclophane Chromophore. *J. Am. Chem. Soc.* **1998**, *120*, 9188−9204.

(24) Boekelheide, V. Synthesis and Properties of the [2_n]-Cyclophanes. *Top. Curr. Chem.* **1983**, *113*, 87−143.

(25) Spanget-Larsen, J. Electronic States of the [2_n]Cyclophanes. *Theor. Chim. Acta* **1983**, *64*, 187−203.

(26) Ron, A.; Schnepp, O. Electronic Spectrum of 2,2′-Paracyclophane. *J. Chem. Phys.* **1962**, *37*, 2540−2546.

(27) Nurmukhametov, R. N.; Shapovalov, A. V.; Sergeev, A. M. Absorption and Luminescence Properties of [2.2]Paracyclophane due to Strong Transannular Interaction. *J. Appl. Spectrosc.* **2014**, *81*, 49−56.

(28) Dodziuk, H.; Vetokhina, V.; Hopf, H.; Luboradzki, R.; Gawel, P.; Waluk, J. Electronic States of Cyclophanes with Small Bridges. *J. Chem. Phys.* **2012**, *136*, No. 074201.

(29) Demissie, T. B.; Dodziuk, H.; Waluk, J.; Ruud, K.; Pietrzak, M.; Vetokhina, V.; Szymański, S.; Jaźwiński, J.; Hopf, H. Structure, NMR and Electronic Spectra of [*m.n*]Paracyclophanes with Varying Bridges Lengths (*m*, *n* = 2−4). *J. Phys. Chem. A* **2016**, *120*, 724−736.

(30) Meyer-Eppler, G.; Sure, R.; Schneider, A.; Schnakenburg, G.; Grimme, S.; Lützen, A. Synthesis, Chiral Resolution, and Absolute Configuration of Dissymmetric 4,15-Difunctionalized [2.2]-Paracyclophanes. *J. Org. Chem.* **2014**, *79*, 6679−6687.

(31) Langer, E.; Lehner, H.; Schloegl, K. Eine Beziehung Zwischen Absoluter Konfiguration und dem ^1L_b-Cottoneffekt Chiraler Carbophane. *Tetrahedron* **1973**, *29*, 2473−2478.

(32) Furo, T.; Mori, T.; Wada, T.; Inoue, Y. Absolute Configuration of Chiral [2.2]Paracyclophanes with Intramolecular Charge-Transfer Interaction. Failure of the Exciton Chirality Method and Use of the Sector Rule Applied to the Cotton Effect of the C-T Transition. *J. Am. Chem. Soc.* **2005**, *127*, 8242−8243.

(33) Furo, T.; Mori, T.; Origane, Y.; Wada, T.; Izumi, H.; Inoue, Y. Absolute Configuration Determination of Donor-Acceptor [2.2]-Paracyclophanes by Comparison of Theoretical and Experimental Vibrational Circular Dichroism Spectra. *Chirality* **2006**, *18*, 205−211.

(34) Gleiter, R. Consequences of σ-π-Interaction in [2.2]-Paracyclophane. *Tetrahedron Lett.* **1969**, *10*, 4453−4456.

(35) Christiansen, O.; Koch, H.; Jørgensen, P. The Second-Order Approximate Coupled Cluster Singles and Doubles Model CC2. *Chem. Phys. Lett.* **1995**, *243*, 409−418.

(36) Hättig, C. Structure Optimizations for Excited States with Correlated Second-Order Methods: CC2, CIS(D1), and ADC(2). *Adv. Quantum Chem.* **2005**, *50*, 37−60.

(37) Mori, T.; Tanaka, T.; Higashino, T.; Yoshida, K.; Osuka, A. Combined Experimental and Theoretical Investigations on Optical Activities of Möbius Aromatic and Möbius Antiaromatic Hexaphyrin Phosphorus Complexes. *J. Phys. Chem. A* **2016**, *120*, 4241−4248.

(38) Wakai, A.; Fukasawa, H.; Yang, C.; Mori, T.; Inoue, Y. Theoretical and Experimental Investigations of Circular Dichroism and Absolute Configuration Determination of Chiral Anthracene Photodimers. *J. Am. Chem. Soc.* **2012**, *134*, 4990−4997.

(39) Nakai, Y.; Mori, T.; Sato, K.; Inoue, Y. Theoretical and Experimental Studies of Circular Dichroism of Mono- and Diazonia[6]helicenes. *J. Phys. Chem. A* **2013**, *117*, 5082−5092.

(40) Nakai, Y.; Mori, T.; Inoue, Y. Circular Dichroism of (Di)methyl- and Diaza[6]helicenes. A Combined Theoretical and Experimental Study. *J. Phys. Chem. A* **2013**, *117*, 83−93.

(41) Nakai, Y.; Mori, T.; Inoue, Y. Theoretical and Experimental Studies on Circular Dichroism of Carbo[*n*]helicenes. *J. Phys. Chem. A* **2012**, *116*, 7372−7385.

DOI: 10.1021/acsomega.7b01642
ACS Omega 2018, 3, 22−29

(42) Kang, J.; Miyajima, D.; Mori, T.; Inoue, Y.; Itoh, Y.; Aida, T. A Rational Strategy for the Realization of Chain-Growth Supramolecular Polymerization. *Science* **2015**, *347*, 646−651.
(43) Tanaka, H.; Inoue, Y.; Nakano, T.; Mori, T. Absolute Configuration Determination through the Unique Intramolecular Excitonic Coupling in the Circular Dichroisms of *o,p′*-DDT and *o,p′*-DDD. A Combined Experimental and Theoretical Study. *Photochem. Photobiol. Sci.* **2017**, *16*, 606−610.
(44) Seino, J.; Honda, Y.; Hada, M.; Nakatsuji, H. SAC and SAC-CI Calculations of Excitation and Circular Dichroism Spectra of Straight-Chain and Cyclic Dichalcogens. *J. Phys. Chem. A* **2006**, *110*, 10053−10062.
(45) Autschbach, J.; Nitsch-Velasquez, L.; Rudolph, M. Time-Dependent Density Functional Response Theory for Electronic Chiroptical Properties of Chiral Molecules. *Top. Curr. Chem.* **2011**, *298*, 1−98.
(46) Duncan, W. T.; Truong, T. N. Thermal and Vibrational-State Selected Rates of the CH_4 + Cl ↔ HCl + CH_3 Reaction. *J. Chem. Phys.* **1995**, *103*, 9642−9652.
(47) Zhao, Y.; Truhlar, D. The M06 Suite of Density Functionals for Main Group Thermochemistry, Thermochemical Kinetics, Noncovalent Interactions, Excited States, and Transition Elements: Two New Functionals and Systematic Testing of Four M06-Class Functionals and 12 Other Functionals. *Theor. Chem. Acc.* **2008**, *120*, 215−241.
(48) Yanai, T.; Tew, D. P.; Handy, N. C. A New Hybrid Exchange-Correlation Functional Using the Coulomb-Attenuating Method (CAM-B3LYP). *Chem. Phys. Lett.* **2004**, *393*, 51−57.
(49) Kay, K. Y.; Baek, Y. G.; Han, D. W.; Yeu, S. Y. Facile Synthesis of Novel Bis- and Tetrakis(2-ferrocenylvinyl)[2,2]paracyclophanes by Palladium-Catalyzed Coupling Reactions. *Synthesis* **1997**, 35−37.
(50) Bondarenko, L.; Dix, I.; Hinrichs, H.; Hopf, H. Cyclophanes. Part LII: Ethynyl[2.2]paracyclophanes - New Building Blocks for Molecular Scaffolding. *Synthesis* **2004**, 2751−2759.

DOI: 10.1021/acsomega.7b01642
ACS Omega 2018, 3, 22−29